WELDING RESEARCH

SUPPLEMENT TO THE WELDING JOURNAL, SEPTEMBER, 1983
Sponsored by the American Welding Society and the Welding Research Council

Infrared Thermography for Sensing the Arc Welding Process

Arc misalignment, joint geometry faults, variations in penetration and impurities are found to produce distinctly different distributions of weld pool surface temperature

BY B. A. CHIN, N. H. MADSEN, AND J. S. GOODLING

ABSTRACT. A feasibility study was performed to determine if infrared thermography could be used to detect perturbations that result in faults during the arc welding process. An infrared camera, capable of resolving a ±0.2°C (±0.36°F) difference in temperature, was aimed at the weld pool during welding. Several weld errors were then intentionally induced. The resulting images showed that the temperature field is detectably altered in the vicinity of the weld pool. Arc misalignment, groove geometry faults, variations in penetration and impurities were discernible in distinctly different ways.

With the use of computer-aided processing of these images, it is expected that the welding process can be controlled to a higher degree than is presently available.

Introduction

Automatic welding is commonplace in industry today. However, most, if not all, involves preprogramming for performance of a repetitive task. These systems are incapable of correcting for perturbations which arise during the welding process. The number of machine variables (current, position, speed, *etc.*) and workpiece variables (root opening, misalignment, *etc.*) coupled with the need for a technique for near-instantaneous moni-

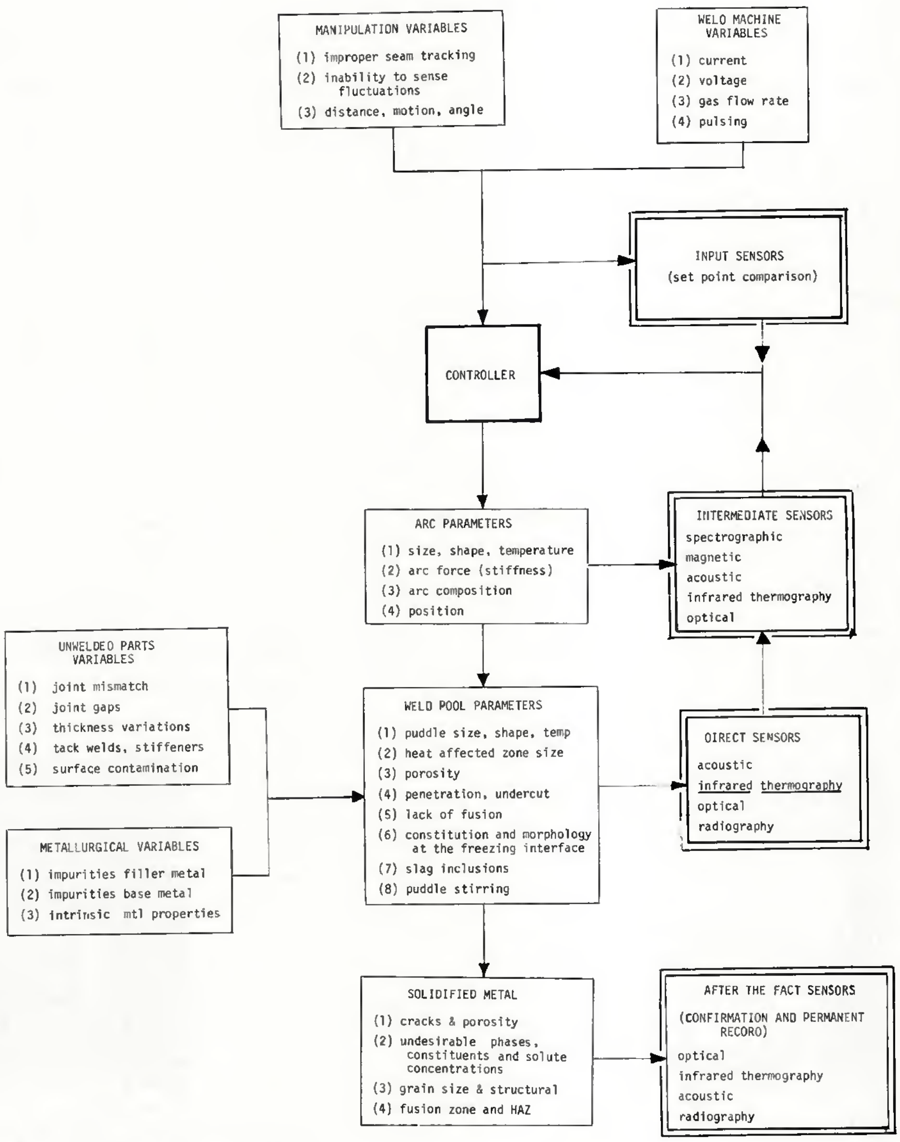

Fig. 1—Welding process diagram

Paper presented at the 64th Annual AWS Convention held in Philadelphia, Pennsylvania, during April 24-29, 1983.

B. A. CHIN is Alumni Associate Professor, N. H. MADSEN is Assistant Professor, and J. S. GOODLING is Professor, Mechanical Engineering Department, Auburn University, Auburn, Alabama.

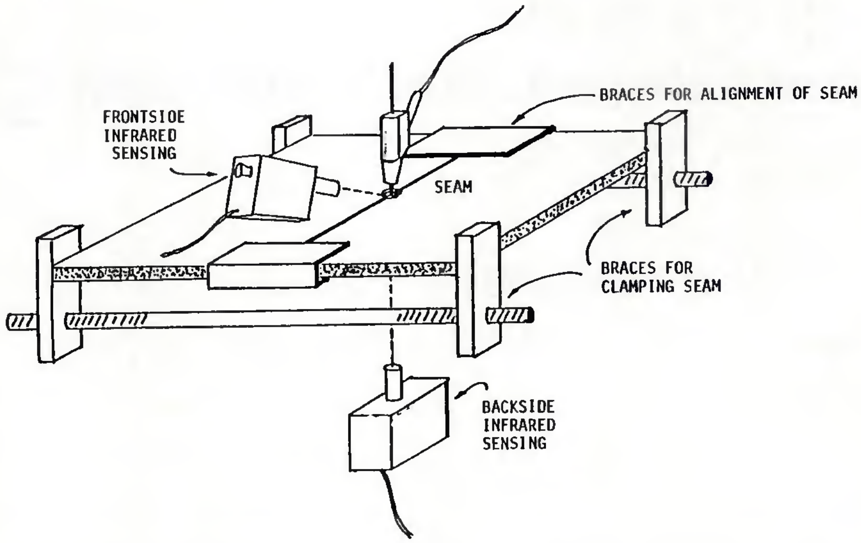

Fig. 2 — Schematic showing restraint of plates and positions of infrared camera and welding arc

toring of these variables, have prevented the successful development of a closed-loop feedback control system for precision welding. This paper presents results that could aid in the assembly of such a controlled system for welding.

The high temperatures associated with arc welding and the appropriate thermophysical properties (primarily thermal diffusivity) of the parts to be welded cause very strong spatial temperature gradients (of over 10^5 °C/m, *i.e.*, 4.6×10^3°F/in.) in the vicinity of the weld pool surface. Modern infrared thermography equipment allows fast sensing of these gradients with a high degree of accuracy.

For a perfect weld these gradients should show repeatable and regular patterns. However, imperfections should cause a discernible change in the thermal profiles. Based on this hypothesis, experiments were carried out to determine the quality and magnitude of the changes as a function of specific induced weld discontinuities, arc or plate misalignment, variations in penetration, and contamination.

Role of Sensors

Since World War II, engineers have been striving to develop fully automatic welding machines. Today, machines have progressed to a state where preprogrammed conditions can be set as a function of time or position. Only a few companies have begun to market systems with limited in-process feedback sensing for applications such as V-groove seam tracking.

Welding automation research has concentrated principally on systems for seam or joint tracking (Ref. 1-6), magnetic control of arcs for positioning (Ref. 7-11), and penetration control through weld pool characterization (Ref. 12-15). Attempts to adapt intelligent vision systems to seam tracking and weld pool control have also been made (Ref. 16-20). Most concepts of welding control have been adapted from computer vision based systems. Ultrasonics (Ref. 21-23), acoustic emission (Ref. 24-26), and infrared temperature (Ref. 27-32) sensing systems have also been used as sensors, primarily as after-the-fact inspection devices. Recently, infrared thermography has been used to monitor cooling rates in welds as a possible means of on-line control of heat input (Ref. 33).

Although the above research has led to increased knowledge of arc welding physics, an acceptable sensing system for in-process welding and quality control has not been developed. The development of improved sensors is required to achieve wide scale automation of the welding process.

A flow diagram of the welding process showing input variables and conditions which can be monitored for feedback control is shown in Fig. 1. The unwelded part variables and metallurgical variables are the input conditions over which direct feedback control is not exercised. However, other welding variables such as welding machine current and arc manipulation (weaving, travel speed, and positioning) may be altered to compensate for fluctuations in these inputs. Welding machine variables and manipulation variables can be directly controlled in the process and provide the principal inputs through which primary in-process control can be exercised.

As indicated in Fig. 1, there are several places in the process where sensors may be used to gather information. The sensors fall into four basic categories based upon their time sequence in the process. These categories are:

1. Input sensors.
2. Intermediate sensors.
3. Direct sensors.
4. After-the-fact sensors.

Input sensors monitor input conditions such as welding machine settings (current, voltage, shielding gas composition and flow rate) and set point manipulation (anticipated position) for random deviation from preprogrammed values. Input sensors consist primarily of instantaneous electrical and flow rate monitors. The need for input sensors may be eliminated as intermediate and direct sensors are developed with sufficient discretionary capabilities (ability to determine the source of a deviation) and adequate time response to decipher and compensate for weld disturbances.

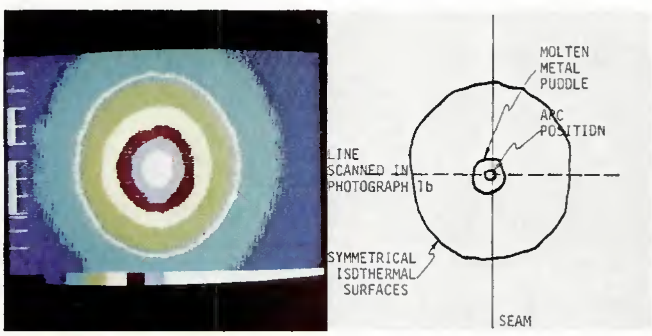

Fig. 3 — Two dimensional thermal scan of plate surfaces. Temperature distribution is symmetrical when stationary arc is placed directly over joint center

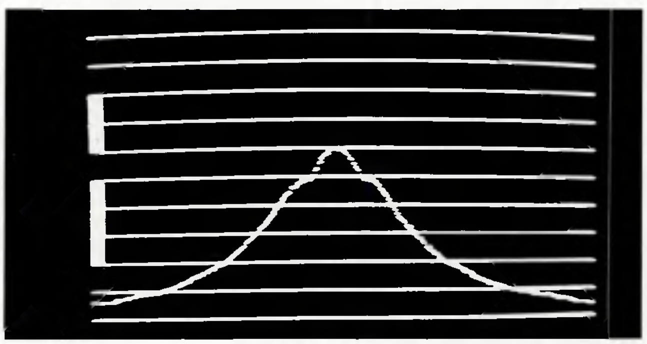

Fig. 4 — Temperature vs. distance scan across center of region shown in Fig. 3. The symmetrical inflections represent the molten metal-solid metal interface

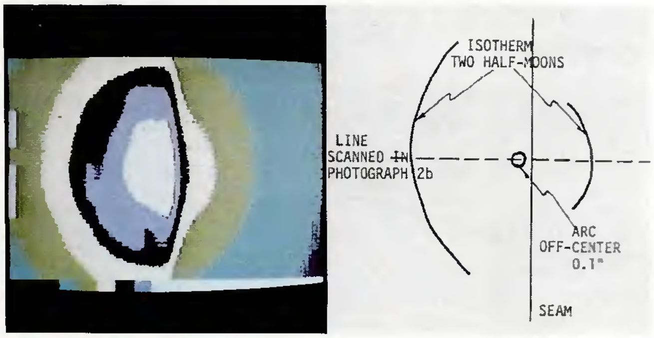

Fig. 5 — Effect of arc position. Arc positioned 0.1 in. (2.5 mm) off-center. Half-moons of different diameter form, yielding a nonsymmetric temperature distribution

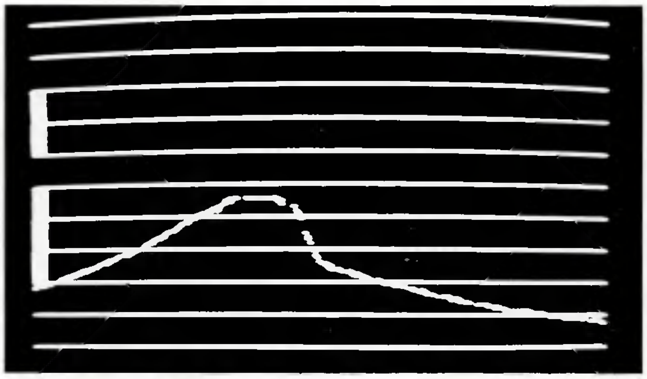

Fig. 6 — Nonsymmetric temperature vs. distance scan across center of region shown in Fig. 5. Temperature distribution becomes highly nonsymmetric around peak temperature

Intermediate sensors monitor the stability of the process. In other words, they search for fluctuations in the shielding gas composition, current, voltage or arc temperature which are indicative of an impending discontinuity. Arc measurements such as size, shape and temperature are examples of intermediate process characteristics which are controllable. This category may consist of spectrographic, magnetic, acoustic, infrared and optical sensors.

Spectrographic sensors would monitor arc plasma composition, revealing deviations in gas composition and possible impending weld porosity from vaporized surface contaminants. Magnetic flux sensors could be used to monitor arc stiffness and control arc position by application of an external magnetic field. Monitoring of acoustic plasma emissions and infrared characterization may enable precise temperature control of the arc.

The third category of sensors provides direct information on the melting and solidification process. Weld pool size, shape and temperature distribution are examples of characteristics that direct sensors would monitor. The input sensors, intermediate sensors and direct sensors have the capability of revealing fluctuations and variations in the process which may lead to the formation of a discontinuity. After-the-fact sensors provide only confirmation and a permanent record of the weld condition prior to placement in service.

The direct sensors will provide the greatest information for control of the welding operations. These sensors monitor the final stage in the process from which information can be fed back to compensate for variations. The direct sensors will provide the best control over the metallurgical melting and freezing process and the clearest signal of an impending defect or undesirable metallurgical structure.

Acoustic, infrared thermography, optical and on-line radiography are methods which could be used to characterize direct welding conditions. However, based upon experimental results presented in this paper, infrared thermography appears to be the most promising of these methods. The plate temperature distribution, as monitored by infrared thermography, will provide information for seam tracking, identification of plate geometry faults, penetration control, contamination and microstructure formation.

Experimental Procedure

To demonstrate the feasibility of using infrared thermography to detect and identify various impending weld problems, a set of experiments was performed. The results of these experiments are detailed below. The experiments were conducted using infrared imaging equipment made by Inframetrics Corporation. The objectives of the experiments were:

1. To determine the sensitivity of the thermal field and infrared detector to geometric variations, arc position, contaminants, penetration depth, and welding machine settings.
2. To determine the time required to identify changes in weld status.

The infrared thermography equipment consisted of a single waveband (8-12 microns) infrared detector, processing and color enhancement system with isothermal line scan, 3X telescope system, attenuator filters, video tape recorder, Polaroid camera and color monitor. The instrument, manufactured by Inframetrics, is capable of measuring temperatures from −20° to 2500°C (−4 to 4532°F). The manufacturer claims that the instrument is capable of resolving temperature differences of ±0.2°C (0.36°F).

All experiments were conducted using 12 × 12 in. (305 × 305 mm) plain carbon steel plates (AISI 1040) ranging in thickness from 0.275 to 0.325 in. (7 to 8.3 mm). The edges to be joined were milled for a precise fit. A Miller model 330A/BP-AC/DC welding unit with water-cooled torch and a 3/16 in. (4.76 mm) diameter tungsten electrode was used to produce the welds. Arc currents between 20 and 150 A at 30 VDC with Ar shielding gas were used. The torch was mounted to a precision positioning table allowing movement in three orthogonal directions — Fig. 2. Movements were controllable to within ±0.01 in. (0.25 mm).

After the initial stationary arc experiments, penetration was maintained between 80 and 95% to assure that no melt-thru occurred that might have damaged monitoring equipment placed on the opposite side of the plates. Torch travel speeds between 2-10 ipm (0.85-4.2 mm/s) were investigated. Only minor spatter and arc reflection problems were encountered. Proper positioning of the camera eliminated these problems.

Experimental Results

Plate Surface Measurements

Initial measurements were made using a stationary arc positioned at the joint between two plates. The plates were clamped tightly together as shown in Fig. 2 to restrain motion due to thermal expansion. Root side measurements were investigated first to avoid molten metal splatter, frontside positioning and arc reflection problems.

Figure 3 is the resulting two dimensional thermal scan with the arc positioned within ±0.01 in. (0.25 mm) of the joint center. The color bar at the bottom of the photograph shows the color assignment to regions of temperature ranging from blue (coolest temperature) to white (hottest temperature). Specific colors may be programmed to represent almost any range of temperatures desired. For instance, the blue color can be preprogrammed to represent temperatures from 600 to 650°C (1112 to 1202°F) and yellow from 900 to 1000°C (1652 to 1832°F). The white circle separating the green and blue regions represents an

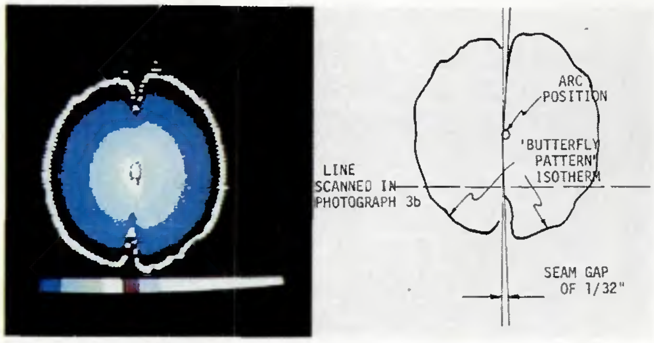

Fig. 7—Effect of joint gap. Arc positioned slightly off center. Gaps shown by dips in isothermal surfaces (exterior white line)

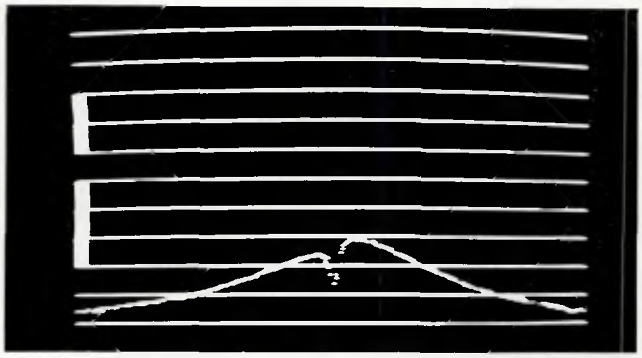

Fig. 8—Temperature vs. Distance Scan Across Bottom of Fig. 7. Two peaks about the plate gap can be seen. These peaks surround the gaps in the plates. The peaks are not of the same height, indicating that the arc is slightly off-center to the right

isothermal profile on the surface. Any temperature can be selected and the isotherm plotted on the two dimensional scan.

Figure 4 is a thermal line scan of Fig. 3 in which temperature is plotted vs. distance across the center of Fig. 3. The distribution is symmetrical, indicating positioning of the arc over the center of the joint. From this profile, one can also determine the average diameter of the weld pool. The inflections around the peak represent the isothermal band of the molten metal-solid metal interface.

Figures 5 and 6 show the temperature distribution which results when the arc is positioned 0.1 in. (2.5 mm) to the left of the center of the joint. The two dimensional thermal scan of Fig. 5 is composed of half-moon shapes or portions of circles. This asymmetrical temperature distribution is caused by contact resistance at the joint. The degree to which the arc is off-center appears to be proportional to the difference in the radii of the half-moons of the isotherms. The temperature distance profile shown in Fig. 6 shows that the temperature distribution is highly nonsymmetrical about the peak temperature.

A marked difference in the thermal distribution symmetry for an arc placed on the joint vs. a placement at a distance of 0.1 in. (2.5 mm) off center is seen by comparing Figs. 3 and 4 to Figs. 5 and 6. The results obtained tend to indicate that seam tracking may be based on the difference in radii of isothermal curves to the left and right of the seam. A simple linear control action could be used to move the arc until both radii were equal.

In addition to seam tracking, the infrared sensors should be able to identify geometrical variations encountered in the welding process such as variations in the joint opening and mismatches. Figures 7-9 show the resulting two dimensional thermal distributions. The variations in the joint opening cause an indentation in the constant temperature lines corresponding to a decrease from the peak temperatures of the metal surrounding the opening.

Figure 7 shows indentations that yield a "butterfly pattern" thermal surface. Figure 8 shows this drop in the temperature-distance profile in a region toward the bottom of Fig. 7. The sensitivity of the infrared sensor in identifying both joint openings and arc position is also shown in these photographs. The half-moons would be of the same size if the arc were positioned directly on the joint center. Also the peak temperatures would be of the same height on both sides of the opening in Fig. 8.

Figure 9 shows the effect of plate mismatch on the thermal distribution. Offsetting one end of one plate with respect to the other (as shown in Fig. 10, a schematic of the configuration) causes a shift in the centers of the half-moons. The plate farthest away from the electrode has a half moon whose center is shifted along the joint toward the position where the two plates match.

Weld Pool Measurements

In addition to seam tracking and detection of geometric plate variations, a good feedback controlled welding system should be able to detect problems in the weld pool prior to solidification. Measurements of the thermal distribution of the weld pool were made by using a 3X telescope which was attached to the infrared camera. The camera was placed in the plane of the joint ahead of the arc as shown in Fig. 2. Various impurities were placed in the joint and the arc positioned over these impurities.

A close-up of the weld pool is shown in Figs. 11 and 12. Figure 11 is the two-dimensional temperature distribution of the weld pool with the arc positioned in the center of the joint. Temperature distributions in the weld pool oscillate due to motion of the liquid metal but are symmetrical in nature. When impurities such as tungsten were welded over,

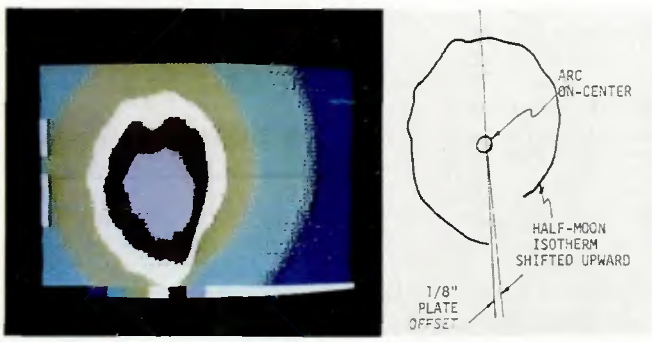

Fig. 9—Effect of plate mismatch. One plate is offset relative to the other. A shift in the position along the joint of the half-moon centers is seen. The plate farthest away from the arc has half-moon isotherms which are shifted toward the position where the plates match

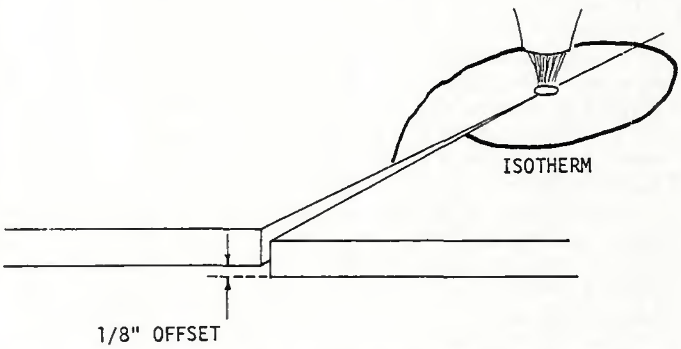

Fig. 10—Schematic of plate configurations and resulting isotherms shown in Fig. 9

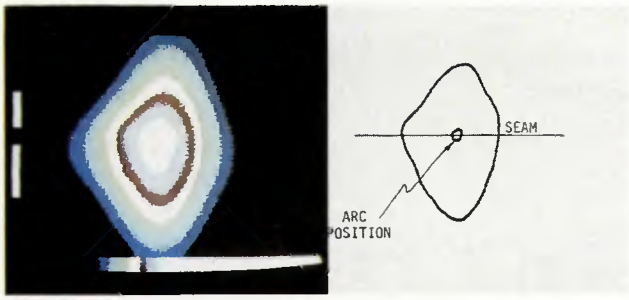

Fig. 11 — Weld pool — no impurities. Symmetric temperature distributions in the molten metal pool were achieved with arc positioned along the joint center. No impurities in puddle

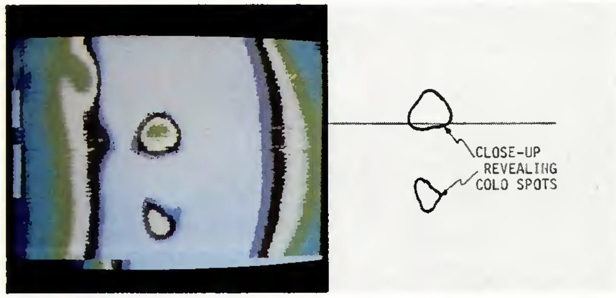

Fig. 12 — Weld pool — impurities. Tungsten impurities placed in the joint cause cold spots in the molten pool shown by dots in the light blue regions

"cold spots" formed in the molten pool as shown by Fig. 12. Identification of such "cold spots" in the weld pool could be used to initiate a slowdown in the traverse speed and pulsing of the arc to mitigate or reduce the undesirable effects.

Measurements were also taken to determine the effect of current (penetration depth) on the temperature profiles. It was found that decreasing the current by ⅓ from the value required for complete joint penetration led to a decrease by ¼ in both penetration depth and radius of the measured isotherm on the surface.

Moving Arc Measurements

The final experiments that were conducted involved the measurement of temperature distributions produced by a moving arc. The camera was positioned for measurements of the face of the joint as in Fig. 2 and the arc moved at a speed of 2.0 ipm (0.85 mm/s) down the joint between two matched and fully restrained plates. Figure 13 shows the thermal distribution which results when the arc is centered on the joint. A parabolic shape of the thermal distribution is obtained which is symmetrical about the joint center. When the arc is shifted off-center by 0.1 in. (2.5 mm), the thermal distribution in Fig. 14 is obtained. As in previous stationary arc cases, the temperature distribution is nonsymmetrical.

Joint gaps ($\leq$ 0.02 in., *i.e.*, 0.51 mm) were also readily detectable in the infrared thermal image. In Fig. 15 the gap is detectable as much as 1.5 in. (38 mm) in front of the arc center (based on field of view calculations). Monitoring thermal distributions at a distance in front of the weld pool allows one to "preview" upcoming plate geometry variations, contaminants and joint position.

Using this technique of previewing thermal distributions, Figs. 16-18 show the ability to identify joint position and contaminants. Sequential Figs. 16 and 17 show the effect of a zig-zag joint on the thermal distribution. As the torch approaches the shift, the isotherm (dark blue) is offset toward the upcoming joint. Similar results were obtained for other joint configurations such as 30 and 45 deg angles.

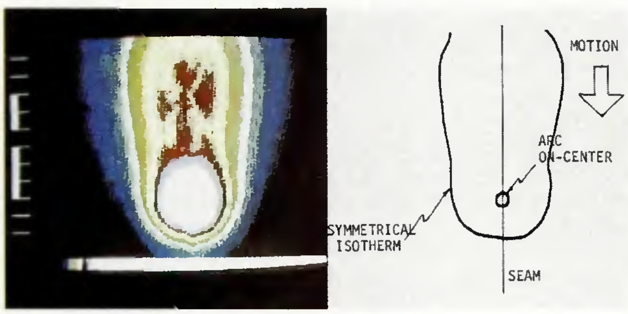

Fig. 13 — Symmetric moving arc temperature distribution. Arc traversing down joint center at a rate of 2.0 ipm (0.85 mm/s)

Fig. 14 — Nonsymmetric moving arc temperature distribution. Arc traversing down the joint, 0.1 in. (2.5 mm) off-center

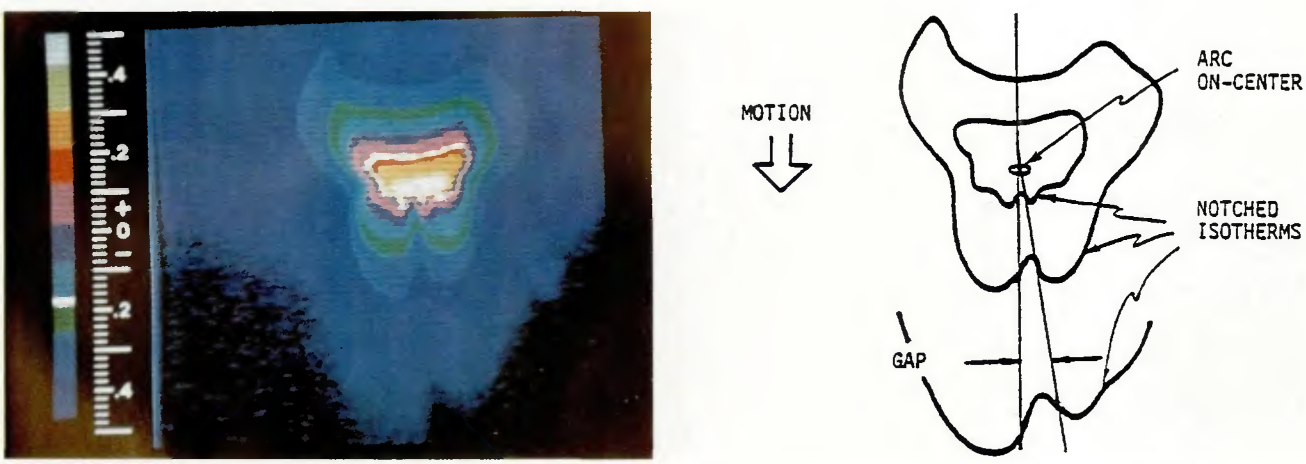

Fig. 15 — Effect of plate gaps on moving arc temperature distribution. The plate gap is indicated by the notches in the color boundaries (isotherms). Note how far ahead of the arc the gap can be detected

Table 1—Summary of Experimental Results

Type of arc	Weld fault	Fig. no.	Thermal field description
Stationary	None	3,4	Symmetrical isotherms
	Arc misalignment	5,6	Asymmetrical half-moons
	Joint gap	7,8	Symmetrical half-moons with distinct indentations at gap
	Plate mismatch	9	Half-moon centers shifted along seam
	Impurities	11,12	Cold spots in weld pool
Moving	None	13,14	Symmetrical trailing isotherms
	Joint gap	15	Near-symmetrical trailing isotherms with leading indentations
	Zig-zag joint	16,17	Leading isotherm shifts sequentially
	Impurities	18	Cold spot in weld pool

Contaminants can also be detected for moving arc cases. In Fig. 18, the impurity is seen as a closed "cold spot," not unlike similar spots seen in Fig. 12. This temperature distribution resulted from a 0.0625 in. (1.59 mm) diameter Al_2O_3 particle which was placed along a joint being traversed by the arc at a speed of 2 ipm (0.85 mm/s). The particle becomes clearly visible as much as 1.5 in. (38 mm) ahead of the arc center.

Discussion of Results

The experimental results are summarized in Table 1. As can be seen, each weld fault creates its own distinctive and discernible pattern of isotherms on the plate surface. Further, the characteristics of a stationary arc are similar to those of a moving arc except that the isotherms trail out behind the moving arc. It is also apparent from the results that previewing thermal distributions ahead of the weld pool is an important characteristic which will allow longer times for identification and correction of weld process perturbations.

Simple corrective actions for penetration control and seam tracking are suggested by the symmetry characteristics of the thermal distribution. For instance, control of the size of a specific temperature isotherm (width or distance between temperature inflections of Fig. 4) could be used to control weld pool shape and hence penetration. Similarly, measurement of the distance from arc center to a fixed temperature isotherm in front of the pool (opposite sides of the joint) could be used for seam tracking. From the results presented, there appears to be a direct relation between the degree of arc misalignment and the radii of isotemperature half-moon surfaces.

The entire thermal distribution is not required for all aspects of weld process control. For instance, monitoring the temperature at two fixed positions in front of the arc may be all that is required for seam tracking of symmetrical geometry parts. Additionally, because of the distinct temperature distributions achieved, it is anticipated that integration of all weld perturbation sensors into one large control sequence may not be required.

Non-coupled logic routines for specific corrective actions are envisioned. For instance, arc positioning involves identifying plate temperature symmetry and moving the arc in a horizontal plane. Such action would be independent of weld pool fault control; it would involve identifying weld pool characteristics and, for instance, current pulsing for puddle agitation and redistribution of contaminants.

There were two areas of interest that were not investigated in depth in these preliminary experiments. They are both germane to infrared sensed welding and are discussed here briefly; they are emissivity and time required to determine temperature fields over areas of concern.

Emissivity

Measurement of absolute temperatures by infrared thermography requires that the emissivity of the radiating surfaces be known. In the experiments which have been described, the principal interest was on relating patterns of the temperature distribution field to various geometric perturbations such as variations in root opening, mismatch and arc position. These experiments have relied on an analysis of symmetry or the lack of symmetry about the joint. As such, a detailed knowledge of the surface emissivity was not required.

To obtain the greatest amount of information about the welding process from the infrared sensors, it would be advantageous to know both absolute temperature and emissivity as a function of position. This information could be used to monitor temperature history of the plates for microstructure control and to identify surface contaminants. Unfortunately, most metals are poor emitters of infrared radiation, their reflectivity being high at high temperatures. The emissivity of the metal surface is also dependent on its condition (rough, oxidized, *etc.*). Coatings can be used to provide the specimen surface with a high uniform emittance. However, differences in coating thickness and bonding can result in erroneous measurements.

Techniques have been developed that reduce the problems associated with variable surface emissivities. These techniques have been successful in nondestructive testing of nuclear fuel pin welds (Ref. 30). These techniques—known as Emittance Independent Infrared Analysis (EIIA)—involve the simultaneous scan of

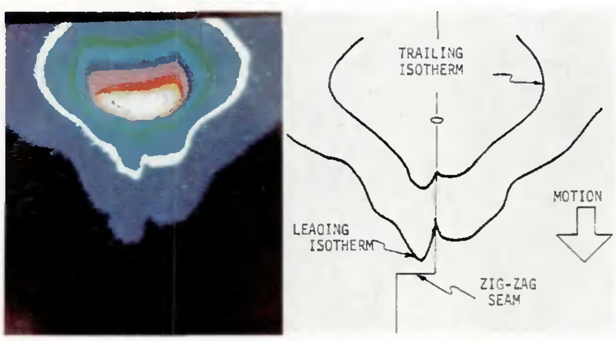

Fig. 16—Seam tracking—straight portion. The isotherms indicate that the joint immediately ahead of the arc is straight

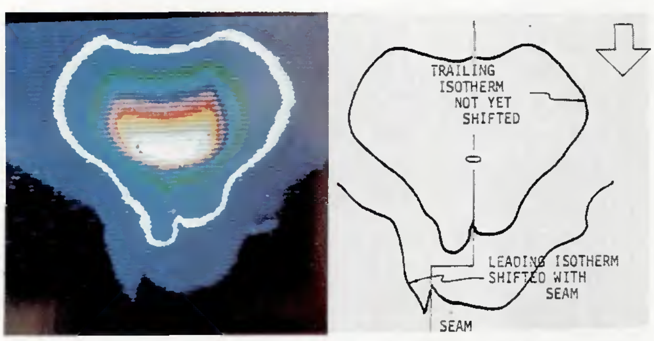

Fig. 17—Seam tracking—shifted portion. The leading isotherm indicates the upcoming shift in the joint. This demonstrates that impending tracking errors can be detected

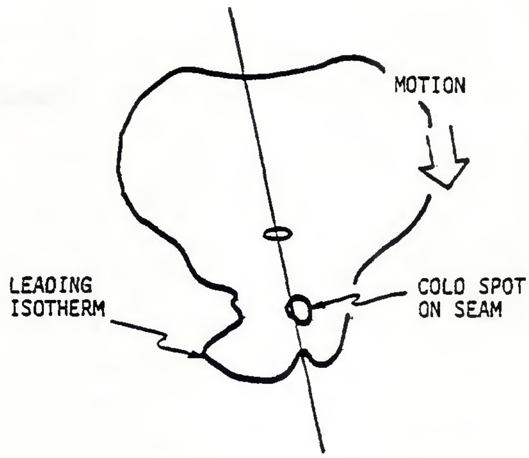

Fig. 18 — Impurities in a moving arc. The small white circle indicates a cold spot ahead of the arc. This was caused by an impurity placed in the weld path

dual infrared detectors.

Changes in temperature for a surface of constant emissivity result in both a change in intensity (more area under the curve) and distribution (shift of peak intensity). However, emittance variations affect principally the intensity and not the distribution (assuming gray-body behavior). If the intensities at two wavelengths are simultaneously measured over the same area of the target, their ratio becomes a function of only the temperature of the target surface. Hence this ratio is independent of emissivity. By monitoring both the absolute values of intensities and the ratios of intensities, changes in emissivity can be detected. These changes in emissivity can be used to identify conditions such as oxidation or surface contamination.

Time/Temperature Field Determinations

The ultimate applicability of infrared thermography to welding process control will depend upon how rapidly weld problems can be detected, identified and appropriate corrective action taken. Detectable changes in the thermal distribution are produced very rapidly by changes in weld conditions. The thermal image changes immediately (to within experimental accuracy) when the arc is moved from a stationary position. Further work will be required to determine the minimum time needed to detect meaningful changes in the temperature distribution.

The time required to determine the temperature field over the area of concern is also important. The scanning time of the infrared detector used in the experiments is 8 milliseconds (a full 100 × 100 matrix scan of the field of view), and it is conservatively estimated to require less than 1 millisecond to transmit the data for processing. It is difficult to estimate the required processing time, since this will be a function of the specific logic which must be performed to identify and initiate corrective sequences. Additional experimentation is needed to determine the diagnostics required.

The time available to generate the desired correction can be estimated from the experimental data of the previous section. Consider the case of a plate gap as was shown in Fig. 15. The arc traverse speed was 2 ipm (0.85 mm/s). If one conservatively assumes that an isotherm located 0.25 in. (6.4 mm) in front of the arc were being monitored (corresponding to the green band in Fig. 15), there would be 7.5 s to identify and respond to the problem. It, therefore, appears that adequate response time exists for plate geometry diagnostics. Similar arguments applied to Figs. 16-18 indicate even longer times are available to respond to joint variations and impurities. Detailed experimentation is required to develop diagnostics. However, the initial results (millisecond detection times and dramatic effects) appear very favorable.

These experiments have demonstrated that infrared thermography can identify the weld problems delineated at the start of this section. The photographs show that geometric variations, arc position, contaminants, penetration depth, and weld machine variables can all be detected within a time frame consistent with automatic control of the welding process. It is expected that the use of a dual scanning system will permit control over surface contaminants and material microstructure. These characteristic temperature distributions may be the missing link required for integration with computer-aided processing to permit closed-loop control of the welding process.

Conclusion

Specific weld faults were intentionally induced into an arc welding process, and the resulting surface isotherms were observed using a scanning infrared camera for both stationary and moving arcs. Each fault produced a distinctively different distribution of the surface temperature. The infrared camera is capable of monitoring arc position relative to the seam and can be used to identify plate geometry faults such as plate gaps and offset. Changes in the patterns of surface isotherms in front of a moving arc are directly related to depth of penetration, impurities and obstructions. Faults as small as 1/32 in. (0.8 mm) in diameter can be observed in the weld pool prior to solidification. It appears, therefore, that infrared thermography can be used as a sensor for incorporation into a closed loop feedback system for continuous process and quality controlled welding.

References

1. Moorhead, A. J., and Reed, R. W. 1980. Internal bore welding of 2 1/4 Cr-1Mo steel tube to tubesheet joints. *Welding Journal* 59(9):41-50.

2. Nozaki, T., and Higo, Y. 1980. The development of an arc welding robot for shipbuilding. *Joint Automatic Control Conference,* FA7-A.

3. Cook, G. E. 1980. Feedback control of process variables in arc welding. *Joint Automatic Control Conference,* FA-7, B.

4. Edmonds, D. P., Goodwin, G. M., and Slaughter, G. M. 1977. Development of automated pipe and tube welding techniques for aluminum. *Welding Journal* 56(2):22-25.

5. Houldcraft, P. T. 1966. Automation and automatic welding. *British Welding Journal* 13(4):212.

6. Bollinger, J. G., and Harrison, H. L. 1971. Automated welding using spatial seam tracing. *Welding Journal* 50(11):787-792.

7. Bachelis, J. A., *et al.* 1966. Movement of the electric arc in a magnetic field. *Automatic Weld.* 19(4):43.

8. Mandelberg, C. L., *et al.* 1976. Control of arc welding with the help of a traveling magnetic field. *Automatic Weld.* 29(9):1.

9. Hicken, G. K., Stucki, N. D., and Randall, H. W. 1976. Application of magnetically con-

trolled welding arcs. *Welding Journal* 55(4):264-267.

10. Jayarajan, T. N., and Jackson, C. E. 1972. Magnetic control of gas tungsten arc welding process. *Welding Journal* 51(8):377-s to 385-s.

11. Guile, A. E. 1970. Magnetic fields in arc welding. *IEEE Conference on Gas Discharges*, no. 70: 489.

12. L'vov, M. S., and Igoshin, A. P. 1971. A system for automation of arc welding with self adjustment by depth of penetration. *Automatic Weld.* 24(5):42.

13. Naidenov, A. M. 1969. Mechanical control of the transfer of electrode metal. *Automatic Weld.* 22(12):35.

14. Vilkas, E. P. 1966. Automation of gas tungsten arc welding process. *Welding Journal* 45(5):410-416.

15. McCampbell, W. M., *et al.* 1966. Development of weld intelligence system. *Welding Journal* 45(3):139-s to 144-s.

16. Vanderbrug, G. J., Albus, J. S., and Barkmeyer, E. 1979 (March). A vision system for real time control of robots. *Proceedings 9th International Conference on Industrial Robots.* Washington, D.C.

17. Eskenazi, R., and Wilf, J. M. *Low level processing for real-time image analysis.* JPL report 79-79, NASA contract NAS7-100.

18. Vaisband, Y. S., *et al.* 1970. A television system for automatically guiding electrodes along butt welds. *Automatic Weld.* 24(7):47.

19. Yokoshima, N., and Takagi, H. 1980. Online adaptive control of narrow gap CO_2 welding with industrial television camera. *Joint Automatic Control Conference*, FA7-F.

20. Paton, B. E., *et al.* 1971. The mathematical modelling of welding processes to create systems for forecasting the quality of joints and for optimum control. *Automatic Weld.* 24(7):1.

21. Mech, S. J., and Michaels, T. E. 1977 (July). Development of ultrasonic examination methods for austenitic stainless steel weld inspection. *Materials Evaluation*, p. 61.

22. Alder, L., Cook, K. V., Dewey, B. R., and King, R. T. 1977 (July). The relationship between ultrasonic Rayleigh waves and surface residual stress. *Materials Evaluation*, p. 93.

23. Alder, L., Cook, K. V., Whaley, H. L., and McClung, R. W. 1977 (March). Flaw size measurement in a weld sample by ultrasonic frequency analysis. *Materials Evaluation*, p. 44.

24. Jolly, W. D. 1970 (June). The application of acoustic emission to in-process inspection of welds. *Materials Evaluation*, p. 135.

25. Romrell, D. M. 1973. Acoustic emission weld monitoring of nuclear components. *Welding Journal* 52(2):81-s to 87-s.

26. Kiselevskii, F. N., *et al.* 1971. The automatic analyzing of radiographic pictures of welded joints. *Automatic Weld.* 24(7):10.

27. Ramsey, P. W., Chyle, J. J., Kuhr, J. N., Myers, P. S., Weiss, M., and Groth, W. 1963. Infrared temperature sensing systems for automatic fusion welding. *Welding Journal* 42(8):337-s to 346-s.

28. Green, D. R., and Hassberger, J. A. 1977 (March). Infrared electro-thermal examination of stainless steel. *Materials Evaluation*, p. 39.

29. Green, D. R. 1979. Experimental electro-thermal method for nondestructively testing welds in stainless steel pipes. *Materials Evaluation* 37(11):54.

30. Green, D. R. 1968. Principles and applications of emittance-independent infrared nondestructive testing. *Applied Optics* 7(9):1779.

31. McCullough, L. D., and Green, D. R. 1972. Electrothermal nondestructive testing of metal structures. *Materials Evaluation* XXX(4):87.

32. Malmuth, N. D., Hall, W. F., Davis, B. I., and Rosen, C. D. 1974. Transient thermal phenomena and weld geometry in GTAW. *Welding Journal* 53(9):388-s to 400-s.

33. Lukens, W. E., and Morris, R. A. 1982. Infrared temperature sensing of cooling rates for arc welding control. *Welding Journal* 61(1):27-33.